Structural Basis for Light Activation of a Chloroplast Enzyme: The Structure of Sorghum NADP-Malate Dehydrogenase in Its Oxidized Form[†,‡]

Kenth Johansson,[§] S. Ramaswamy,[§] Markku Saarinen,[§,||] Martine Lemaire-Chamley,[⊥] Emmanuelle Issakidis-Bourguet,[⊥] Myroslawa Miginiac-Maslow,[⊥] and Hans Eklund*[,§]

Department of Molecular Biology, Swedish University of Agricultural Sciences, Biomedical Center, Box 590, S-751 24 Uppsala, Sweden, and Institut de Biotechnologie des Plantes, UMR 8618 CNRS, Bat 630, Université de Paris-Sud, F-91405 Orsay, France

Received December 7, 1998; Revised Manuscript Received February 2, 1999

ABSTRACT: Some key chloroplast enzymes are activated by light via a ferredoxin−thioredoxin reduction system which reduces disulfide bridges in the enzymes. We describe for the first time the structural basis for the redox activation of a chloroplast enzyme, the NADP-dependent malate dehydrogenase (MDH) from *Sorghum vulgare* whose structure has been determined and refined at 2.4 Å resolution. In addition to the normal structural components of MDHs, the enzyme exhibits extensions at both the N- and C-termini, each of which contains a regulatory disulfide bridge which must be reduced for activation. The N-terminal disulfide motif is inserted in a cleft between the two subunits of the dimer, thereby locking the domains in each subunit. The C-terminal disulfide keeps the C-terminal residues tight to the enzyme surface and blocks access to the active site. Reduction of the N-terminal disulfide would release the stopper between the domains and give the enzyme the necessary flexibility. Simultaneous reduction of the C-terminal disulfide would free the C-terminal residues from binding to the enzyme and make the active site accessible.

There are several ways by which enzyme activity is regulated: allosteric control, stimulation and inhibition by control proteins, proteolytic activation, and reversible covalent modification. Of the latter type, phosphorylation and dephosphorylation is the most common process. Redox signaling and regulation has become an area of increasing interest as transcription, translation, apoptosis, and enzymatic activity can be regulated in this way (*1*−*8*). It was first described for the activation of chloroplast enzymes by light through the reduction of disulfides, thereby changing the metabolism to become anabolic (*9*). This redox-regulated covalent modification was later shown to be important for the regulation of transcription (*7*, *8*) by changing the activity of transcription factors fos, jun, and NFκB (*1*−*4*). Thioredoxins are the key transmitters of reducing equivalents to target enzymes.

The redox regulation in plants toward an anabolic state is initiated by the production of reduced ferredoxin by photosystem I in light (Figure 1). Reduced ferredoxin reduces chloroplast thioredoxins via ferredoxin−thioredoxin reductase, and thioredoxins reduce a number of chloroplast enzymes, among them NADP-malate dehydrogenase (see ref *10*). The only structure so far determined for a light-regulated chloroplast enzyme is that of oxidized spinach fructose 1,6-bisphosphatase (*11*). However, in this structure, the regulatory disulfides were not visible; thus, the structural basis for redox regulation is still missing.

NADP-dependent malate dehydrogenase [NADP-dependent MDH (EC 1.1.1.82)] catalyzes the reduction of oxaloacetate to malate in higher plants. In C4 plants such as sorghum and maize, it is located in the chloroplasts of mesophyll cells where the produced malate is exported to the bundle-sheath cell chloroplasts, thus delivering reducing equivalents that are needed for the photosynthetic fixation of carbon dioxide into organic molecules (*12*). Among all the malate dehydrogenases, the chloroplastic NADP-dependent form exhibits the unique property of being strictly regulated by light, while the NAD-dependent MDHs are permanently active (*13*). It is totally inactive in the dark and activated by the ferredoxin−thioredoxin system only when the chloroplasts are illuminated (*10*).

Compared to those of the permanently active NAD-dependent forms, the amino acid sequence of NADP-dependent MDH exhibits sequence extensions at the N-terminus (43 amino acids) and at the C-terminus (17 amino acids) (*14*) (Figure 2). Thiol derivatization and site-directed mutagenesis were used to locate the regulatory disulfides: one in the N-terminal extension (cysteines 24 and 29) and the other in the C-terminal extension (cysteines 365 and 377) (*15*−*18*). A transient Cys24−Cys207 disulfide has also been proposed (*19*). To improve the homogeneity of the protein, we engineered a form truncated by 15 residues at the N-terminus corresponding to the shortest naturally occurring form which still retains the regulatory cysteines, activation features, and kinetic parameters of the native enzyme. This truncated enzyme resulted in crystals that could be used in X-ray diffraction studies.

[†] This work was supported by grants from Swedish Natural Science Research Council and the Swedish Council for Forestry and Agricultural Research (to H.E.).

[‡] The atomic coordinates described in this paper have been deposited in the Brookhaven Protein Data Bank (file name 7mdh).

* To whom correspondence should be addressed. Telephone: 46-18 471 45 59. Fax: 46-18 53 69 71. E-mail: hasse@xray.bmc.uu.se.

[§] Swedish University of Agricultural Sciences.

[||] In fond memory.

[⊥] Université de Paris-Sud.

10.1021/bi982876c CCC: $18.00
Published on Web 03/19/1999

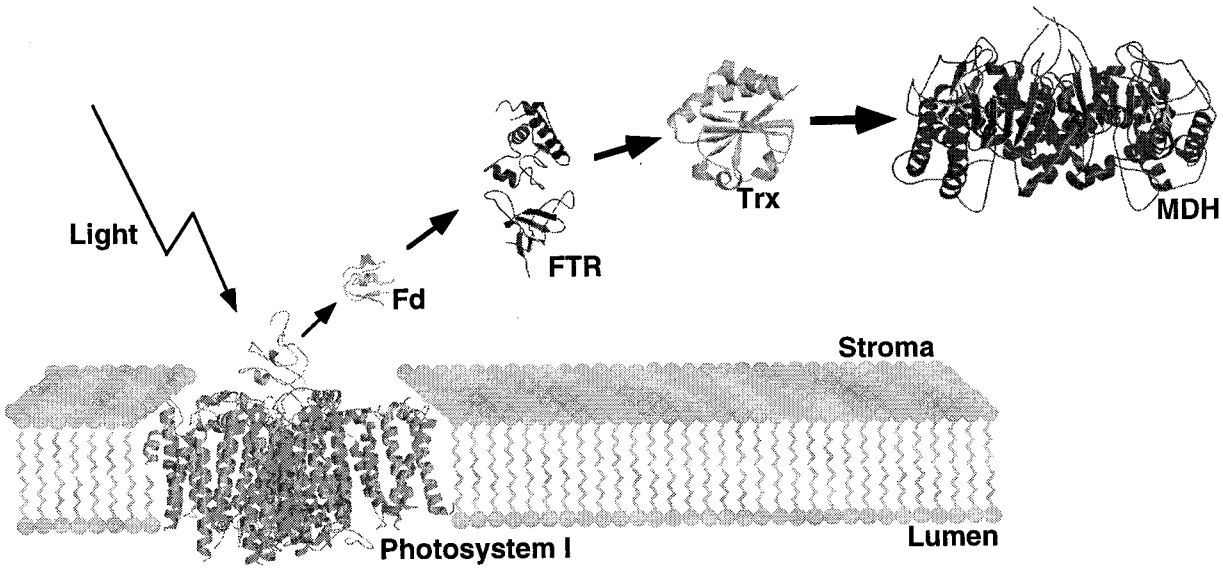

FIGURE 1: Upon illumination, the photosynthetic electron transfer chain reduces ferredoxin by photosystem I. Ferredoxin can then reduce ferredoxin−thioredoxin reductase which reduces thioredoxins. Finally, thioredoxins activate target enzymes, here exemplified by MDH, by reduction of disulfides.

EXPERIMENTAL PROCEDURES

Materials. Restriction endonucleases, T4 DNA ligase, and T4 DNA polymerase were obtained from Appligene. DEAE-Sephacel and Matrex Red A chromatographic supports were from Pharmacia and Grace-Amicon, respectively. Chemicals (purchased from Sigma, Boehringer Mannheim, or Prolabo) were of analytical grade. Oligonucleotides were purchased from Eurogentec and Gibco-BRL, and radiolabels were from Amersham Corp. *Escherichia coli* strain XL1 blue (Clontech) was used to produce high yields of plasmid. *E. coli* strain BL21(DE3) (*20*) and the pET-8c vector (*20*) were used for the production of recombinant NADP-dependent MDH. Bacteria were grown at 37 °C on a Luria broth medium; 50 μg/mL ampicillin was added when the bacteria were carrying plasmids, conferring drug resistance.

Engineering of the mdh cDNA Deleted by 15 Amino Acids at the N-Terminus. The pETmdh-Δ15 vector derived from the previously described pETmdh CM7 vector (*16*) was obtained as follows. The 5′ end of the MDH cDNA was obtained by PCR amplification using oligonucleotides (Eurogentec) with the following sequences: aaaaaccatggaggcgccggcgacgcggaa and cccctgatcagcaaagatttgacc. The *Nco*I−*Apa*I cassette from the PCR product was subcloned into the pETmdh vector and the nucleic acid sequence of the replaced DNA fragment verified by sequencing (*21*) (T7 sequencing kit, Pharmacia).

Production and Purification of Recombinant NADP-Dependent MDHs. The pETmdh-Δ15 vector was used to transform the BL21 *E. coli* strain for high-yield production of the recombinant protein. The experimental procedures for protein production and for the preparation of soluble protein extracts from *E. coli* were like those described previously (*16*). Crude extracts were fractionated by ammonium sulfate precipitation. The precipitate obtained between 35 and 60% saturation was dissolved in 100 mM Tris-HCl (pH 7.5) and 1 mM EDTA and dialyzed overnight against 50 volumes of 20 mM sodium phosphate (pH 7.2) buffer containing 1 mM EDTA (PE buffer). The dialyzed extract was loaded onto a DEAE-Sephacel column (3 cm × 22 cm) equilibrated with PE buffer. After extensive washing with the same buffer, a linear gradient (2 × 250 mL) of 0 to 600 mM NaCl in PE buffer was applied to elute the retained proteins. Fractions enriched in NADP-dependent MDH were pooled and loaded directly onto a Matrex Red A column (1.5 cm × 13 cm). After washing with PE buffer, the enzyme was eluted with a linear gradient of 0 to 3 M NaCl. The fractions containing NADP-dependent MDH activity were pooled and dialyzed overnight against 50 volumes of PE buffer. The dialyzed preparation was concentrated in an Amicon ultrafiltration cell equipped with a YM10 membrane.

Polyacrylamide Gel Electrophoresis. The purity of the preparation was checked by SDS−polyacrylamide gel electrophoresis following the method of Schägger and Von Jagow (*22*). Proteins were visualized by Coomassie Brilliant Blue staining.

Activation and Enzyme Activity Assay. The malate dehydrogenase activity of crude extracts and purified samples was assayed by measuring the decrease in absorbance at 340 nm at 30 °C. The enzyme was activated at 25 °C by preincubation with 20 μM *E. coli* thioredoxin (purified as described in ref *23*) and 10 mM DTT in 100 mM Tris-HCl buffer (pH 7.9). The NADP-dependent MDH activity was measured on aliquots in a standard assay mixture (1 mL) containing 100 mM Tris-HCl (pH 7.9), 780 μM oxaloacetate, and 140 μM NADPH. K_m values for substrates of the activated enzymes were determined by varying the concentration of one of the substrates while keeping the concentration of the other one fixed.

Crystallization and Data Collection. Crystallization trials were carried out by the hanging drop vapor diffusion method at 15 °C. Crystals of sorghum malate dehydrogenase were grown from a solution containing 0.1 M HEPES (pH 7.2), 5% PEG 8000, and 30 mM zinc acetate which was mixed 1:1 with a solution containing 10 mg/mL protein in 0.1 M HEPES (pH 7.2). The crystals belong to orthorhombic space group $C222_1$ and have the following unit cell dimensions: $a = 145.4$ Å, $b = 153.9$ Å, and $c = 160.0$ Å. There are two dimers in the asymmetric unit corresponding to a solvent content of 47%.

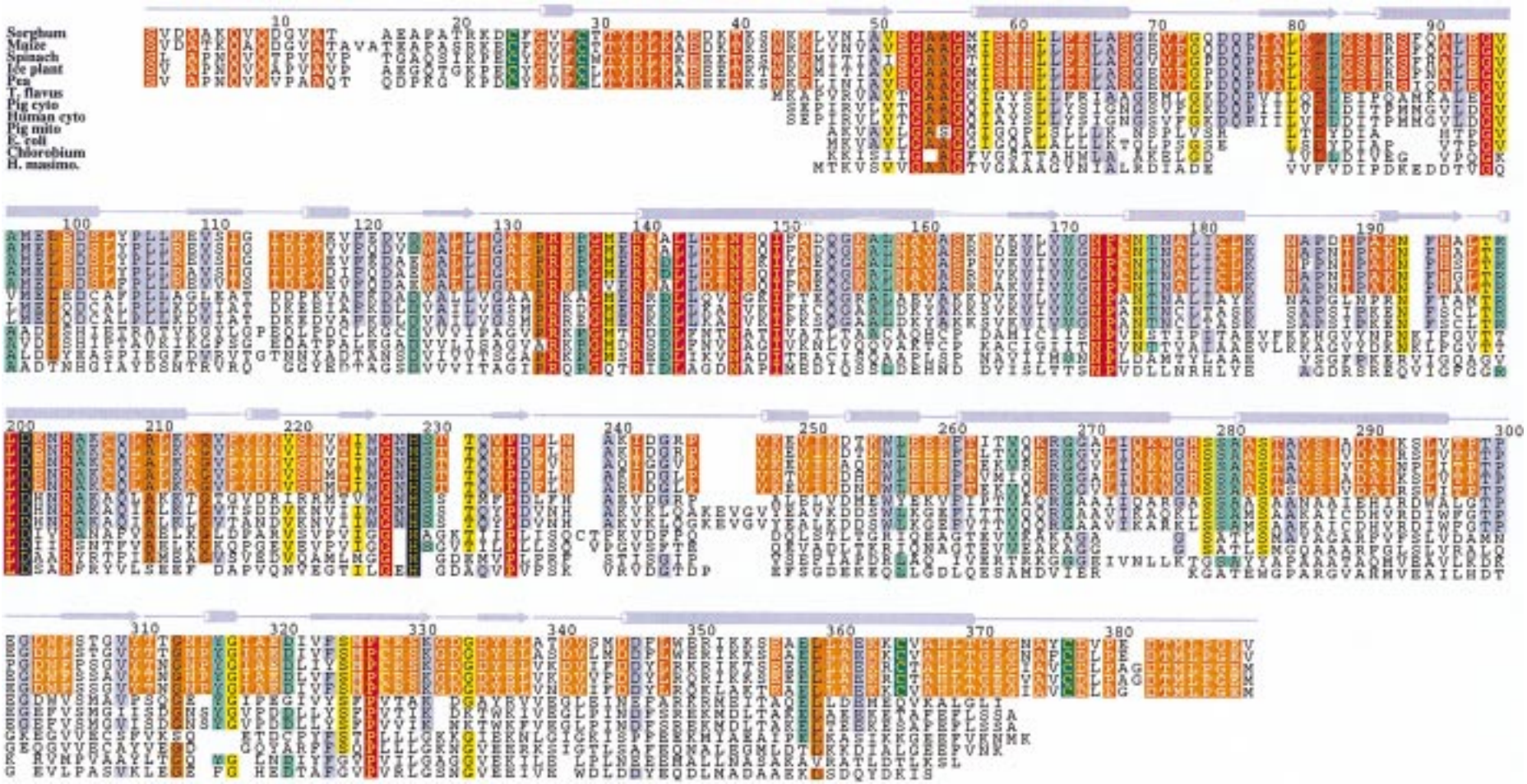

FIGURE 2: Amino acid sequence alignment of MDHs. The chloroplast sequences are highly homologous and have similar extensions at the N- and C-termini. Residues conserved in all chloroplast enzymes are colored orange with white letters, and cysteines in the disulfides in the extensions are colored dark green with white letters. Residues at the active site are colored black with yellow letters. Additional residues which are conserved in all aligned sequences are colored red with white letters. Residues present in all but one of the sequences are colored orange with black letters, and residues present in all but two are colored yellow, in all but three green, and in all but four blue.

The data were collected on beamline 711 at the synchrotron MAX-II in Lund, Sweden, using a MAR345 image plate. The crystals were flash-frozen in a stream of liquid nitrogen at 100 K after a short dip in a cryo solution, consisting of the crystallization buffer and 15% ethylene glycol. The data were indexed, integrated, scaled, and merged using the HKL programs Denzo and Scalepack (*24*).

Structure Solution and Refinement. A model of the sorghum malate dehydrogenase dimer was built previously (*25*) from the coordinates of *Thermus flavus* MDH (PDB file name 1bmd) using the program MODELLER (*26*). This model, with all side chains substituted with alanines, was then used as a search model in molecular replacement. Molecular replacement was carried out using the program AMoRe (*27*).

The model was found to have its overall fold correct, and this allowed us to directly do a round of simulated annealing using CNS (*28*). This resulted in having about 70% of the side chains in the correct position. Initially, strict 4-fold noncrystallographic symmetry (ncs) constraints were used, and molecular averaging, solvent flattening, and histogram matching using DM (*29*) were used to improve the phases. The core of the molecule was built from the average electron density maps; program O (*30*) was used to build the model.

To trace the polypeptide chain in the N- and C-terminal extensions, the programs REFMAC (*31*) and ARP (*32, 33*) were used together. REFMAC was used for energy minimization, and ARP was used to put dummy atoms in positive densities into, initially, averaged $F_o - F_c$ maps. In this way, the entire C-terminal extension (except the last three residues) and parts of the N-terminus were traced.

The ncs restraints were then loosened by applying restraints only to the core of the molecule, i.e., residues 45−365, and letting the extensions be unrestrained. As a final step, a composite omit map of the entire structure was calculated using CNS (*28*) to verify the correctness of the model.

RESULTS AND DISCUSSION

Expression, Purification, and Crystallization. NADP-dependent MDH truncated at the N-terminus (Δ15 mutant) was expressed in bacteria with good yields and was purified by the standard purification procedure set up for the wild-type (WT) enzyme. The pure protein (40−60 mg) was obtained from 10 L cultures. The biochemical properties of the truncated enzyme were compared with those of the unmodfied sorghum enzyme and also with those of a mutant missing the N-terminal disulfide bridge, truncated by 32 amino-terminal residues (ΔN mutant). The results shown in Figure 3 clearly demonstrate that the activation kinetics of the Δ15 mutant are identical to those of the sorghum enzyme (full activation reached after activation with reduced thioredoxin for 5−10 min), whereas the ΔN mutant exhibited the fast activation kinetics typical for MDH without the N-terminal disulfide (*16*). All three activated enzymes had very similar K_m values for substrates (data not shown). Thus, it can be concluded that the short deletion at the N-terminus does not modify the functional properties of the enzyme, and this constitutes a good functional model for the plant protein.

Sorghum MDH was crystallized with the help of zinc ions which form a number of interactions between molecules in the crystal lattice. The crystals of sorghum malate dehydrogenase contain two dimers in the asymmetric unit. The only zinc ions bound within one subunit are at the active site which contains two Zn atoms bound to His229−Asp201 and Cys175−His229, respectively. The coordination spheres are completed in a tetrahedral fashion by water molecules.

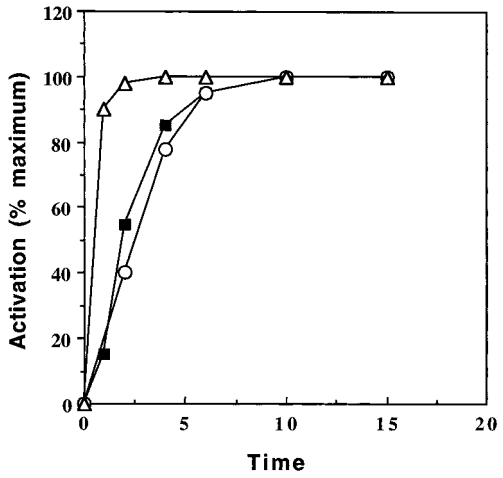

FIGURE 3: Activation time courses of NADP-dependent MDH extracted from sorghum leaves and of deletion mutants Δ15 and ΔN: (■) sorghum NADP-dependent MDH, (○) the Δ15 mutant, and (△) the ΔN mutant. The proteins were preincubated with 20 μmol of recombinant *E. coli* thioredoxin and 10 mM DTT. Aliquots were taken at various preincubation times and their activities measured. The results are expressed as a percentage of the activity of the fully activated enzyme.

Table 1: Data Collection and Refinement Statistics

space group	$C222_1$
cell parameters (Å)	$a = 145.4$, $b = 153.9$, $c = 160.0$
no. of reflections	75861
mosaicity (deg)	0.5
completeness (%)	
all data	94.9
last shell	99.8 (2.40−2.44 Å)
I/σ	
all data	15.1
last shell	4.0 (2.40−2.44 Å)
R_{merge} (%)	6.8
resolution limits (Å)	30.0−2.4
R factor	22
R_{free}	27
average B factor	40.5
Wilson plot B factor	44
rmsd for bond lengths (Å)	0.006
rmsd for bond angles (deg)	1.3

Quality of the Structure. The structure was determined by molecular replacement methods using a model of the sorghum MDH dimer as a search model. The structure was refined to an R value of 0.22 ($R_{free} = 0.27$) with good stereochemistry (Table 1). Most of the residues in the four subunits of the asymmetric unit are in an area of good electron density. The exceptions are primarily related to the N-terminal extensions which have poor density and are evidently flexible. Only the region around the N-terminal disulfide is well-defined. There are two additional regions with poor density. One of these corresponds to the tip of the loop that is flexible in other MDHs and is ordered in MDH complexes with substrate or inhibitor (*34*). The other region is at an external part consisting of residues 272−278.

The core part of the molecule which corresponds to other determined NAD-dependent MDHs is very similar for each of the four subunits in the asymmetric unit with rms

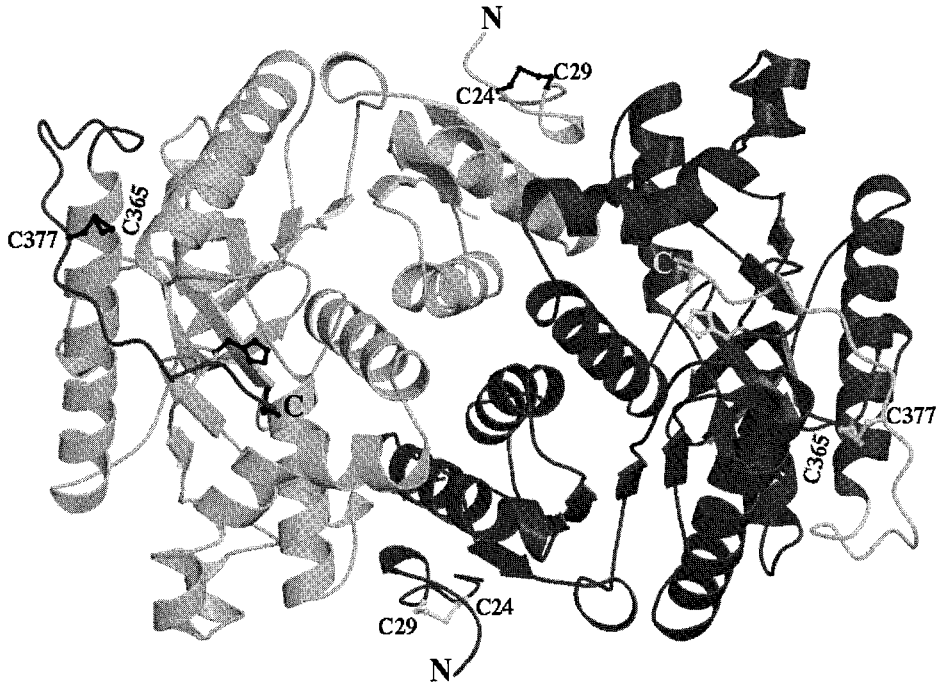

FIGURE 4: Extended N-termini protrude at the top and bottom of the MDH dimer. A disulfide is formed in the oxidized enzyme between Cys24 and Cys29. This part of the N-terminal extension locks the interactions between the coenzyme binding domain of one subunit with the catalytic domain of the other subunit. The C-terminal extension folds back from the edges of the dimer into the active sites. The disulfide bridge between Cys365 and Cys377 stabilizes this conformation. Residues of the N-terminus that are not visible in the electron density are not included in the figure. Therefore, the N-terminal residues in the figure are not connected to the rest of the structure.

differences of <0.5 Å for the core residues plus the C-terminal extension and the region around the N-terminal disulfide bridge (residues 22−32). The residues at the N-terminal side of the disulfide bridge differ considerably between the four subunits and protrude from the protein in different directions.

Overall Structure. The general structure is very similar to those of other malate dehydrogenases, and most of the Cα atoms of the structure can be superimposed with an rms difference of <2 Å on the MDH structures available in the Protein Data Bank (PDB). The secondary structure elements are the same. Most similar to the sorghum enzyme of the MDH structures in PDB is the *T. flavus* MDH for which 634 Cα atoms of the dimer can be superimposed with an rms difference of 1.1 Å. The pleated sheet of the catalytic domain, which differs slightly between MDHs from different species, is also highly similar for sorghum and *T. flavus* MDH (rms difference of 0.6 Å for 150 Cα atoms).

The structure was determined without NADP present, and the binding site contains electron density for water molecules and ions. The adenosine ribose binding site does not contain a carboxylate residue like the NAD-dependent malate dehydrogenases. The corresponding residue in sorghum MDH is instead a glycine which makes space for the extra phosphate group of NADP. The site is surrounded by Ser85, Ser88, and Arg87 which are suitable for NADP binding. As for most MDHs, there is no positively charged residue around the pyrophosphate binding site.

N-Terminal Extension. The extended N-termini protrude from the dimer at the middle of the broad side, while the C-termini come from the outer parts of the longest dimension of the dimer into its center (Figure 4). Both extensions have extended structures except the N-terminal disulfide which forms a short helical structure.

Both disulfide bridges are in an area of well-defined electron density (Figure 5) and confirm that Cys24 and Cys29 form the N-terminal disulfide bridge and Cys365 and Cys377 form the C-terminal disulfide. In the N-terminal disulfide, the cysteines are separated by four residues as in glutathione reductase and related enzymes (*35*), a common motif for disulfides in redox active enzymes. While the residues involved in the disulfide ring break the regular helical structure in glutathione reductase, they form a turn of 3_{10}-helix in MDH with hydrogen bonds between oxygens of residues 25 and 26 and nitrogen atoms of residues 28 and 29, respectively, in NADP-dependent MDH.

The N-terminal disulfide is inserted in a cleft at the subunit interface in the dimer between αC and βC from the same subunit and α2F of the other subunit (secondary structure nomenclature adopted from ref *36*). The Val and the two Phe in the intervening sequence interact in a hydrophobic pocket with Ala96, Met97, Leu99, Leu107, Val110, and Ile112 from the same subunit and Cys207, Leu211, Phe216, and Tyr217 from the second subunit (Figure 6). This N-terminal disulfide part of the structure is also anchored to the enzyme core by three hydrogen bonds: N25···O110 and N27···OE1 of Glu100 and OG1···O108 of Thr31.

N-Terminal Inhibition. If the coenzyme binding domain of subunit A of sorghum MDH is superimposed on the related *T. flavus* enzyme, the coenzyme binding domain of subunit B also can be closely superimposed. However, the catalytic domains differ by a slight domain rotation of about 5°. This may be an effect of the insertion of the N-terminal disulfide part between the two domains. As a consequence, the positions of the active site histidines and aspartic acids differ slightly. Because of the locking of the domains by the N-terminal disulfide, active site residues may not be suitably positioned relative to the coenzyme for catalytic

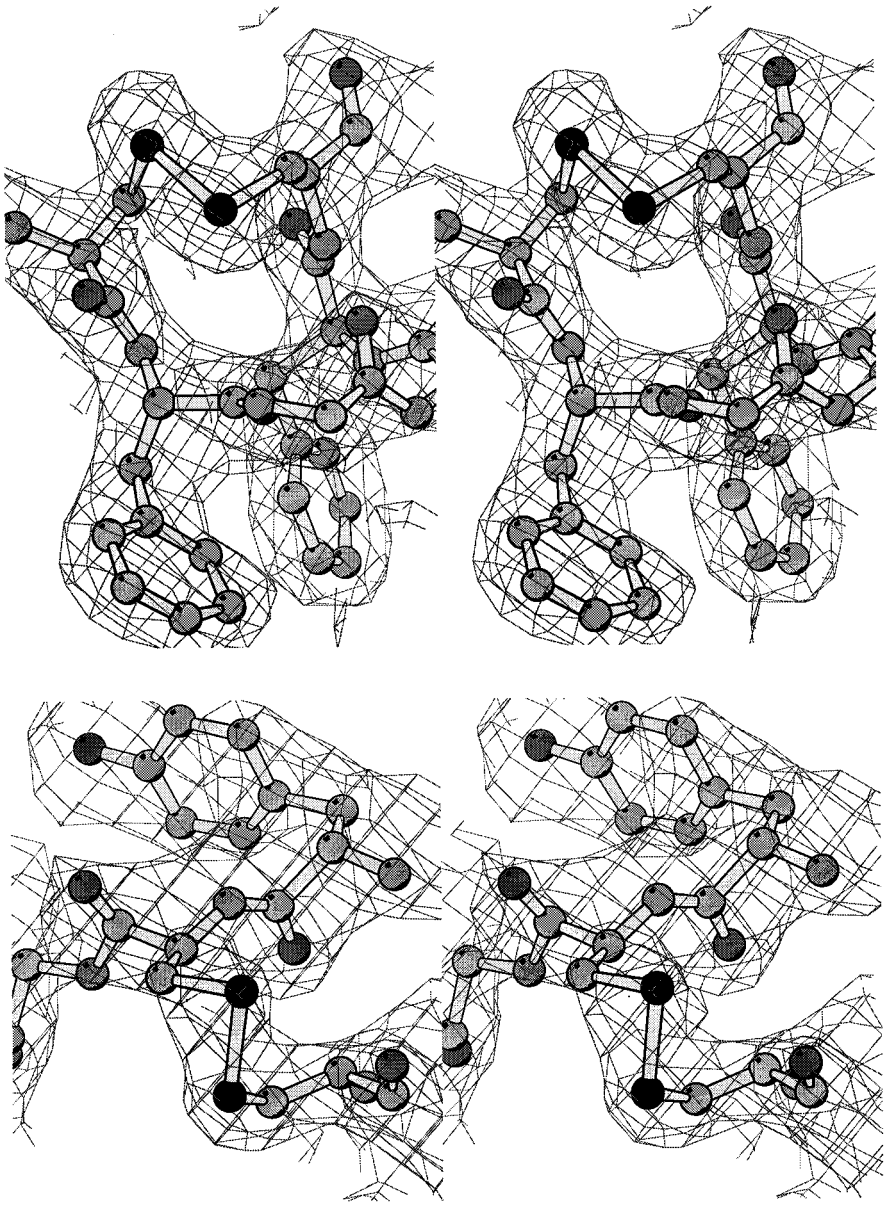

FIGURE 5: Stereoview showing that both disulfide bridges are in areas of well-defined electron density and confirming that Cys24 and Cys29 (top) form the N-terminal disulfide bridge and Cys365 and Cys377 (bottom) form the C-terminal disulfide.

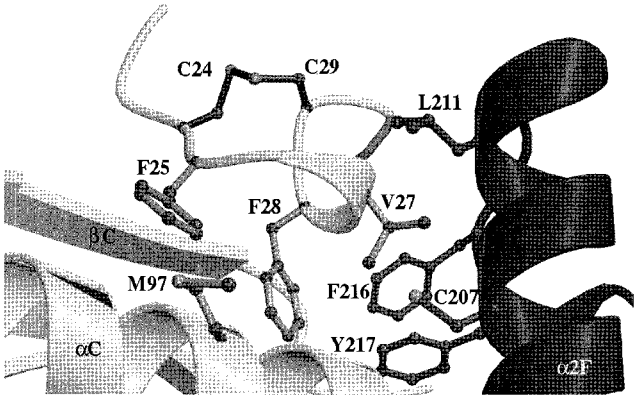

FIGURE 6: Residues in the disulfide structure in the N-terminal extension interact in a hydrophobic pocket with residues from both subunits (light gray and dark gray, respectively).

activity, and therefore, necessary dynamics for the catalytic events are prevented. This may be the reason for the inactivation of the enzyme by the oxidized N-terminal disulfide. Reduction of the N-terminal disulfide should loosen the interactions in the N-terminal extension, but these residues are bound by both hydrogen bonds and favorable hydrophobic interactions in a pocket between the two subunits. The release of the bound residues may still be slow in the reduced form which should mean that the release is the rate-limiting step rather than the conformational change of the relaxed domains.

C-Terminal Extension. The C-terminal disulfide is formed by a residue in the last helix of the MDH core (the helix is present in all MDHs) and a residue in the 17-residue extension which loops back along the helix reaching the active site (Figure 7). The disulfide-forming residues are separated in sequence by 11 residues. The conformation of this bridge is more of a general protein disulfide than a redox active disulfide, where the cysteines generally are separated by two or four intervening residues.

The C-terminal extension makes hydrophobic interactions with the core structure of the protein by Val379, Met384,

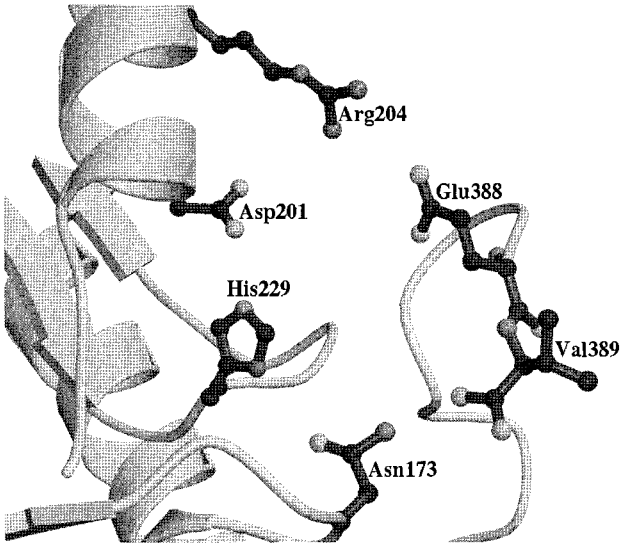

FIGURE 7: C-Terminal residues 388 and 389 in sorghum MDH block the active site. Asn173, Asp201, Arg204, and His229 are conserved residues in MDHs.

and Leu385 and a number of hydrogen bonds from Glu381 to N140 and Arg134 and from Thr383 to N231.

Since the electron densities for the last residues in the molecule were weak, we suspected that the zinc ions which were essential for crystallization also prevented proper binding of the C-terminus to the enzyme. Zn binds between the active site residues with good occupancy under normal crystallization conditions. Testing various conditions for crystallization demonstrated that addition of mercaptoethanol (40 mM) led to conditions under which the crystals were stable, without reduction of disulfides, but with no zinc at the active site. A data set from these crystals showed electron density throughout to the C-terminus. The two last residues in the extension interact with active site residues (Figure 7). An even tighter inhibitory complex is probably formed in the presence of $NADP^+$.

C-Terminal Inhibition. The C-terminus shields the active site. In accordance with recent mutagenesis results (*25*), the structure shows that the C-terminal end of the enzyme is trapped inside the active site, thus supporting the assumption that the last C-terminal residues act as an internal inhibitor of the enzyme.

Activation by Reduction of Disulfides. In the disulfide bridges, Cys29 and Cys377 are exposed and thus are the residues that are accessible to thioredoxin attack. However, thioredoxin-f and thioredoxin-m, as well as *E. coli* thioredoxin, can reduce the disulfides of MDH which means that there is low specificity for the MDH activation. It is rather the availability of reduced thioredoxins in the chloroplasts that is important. Docking studies with different thioredoxin structures demonstrate that the disulfides of MDH are accessible enough for reduction to occur.

The three-dimensional structure of oxidized sorghum MDH is a first step toward understanding the conformational rearrangements during the activation of the enzyme. The second step should be the elucidation of the three-dimensional structure of the activated (reduced) form. However, in view of the flexibility of the N-terminal extension, both extensions can be assumed to be flexible in the reduced structure. The availability of various partially deregulated mutants lacking some of the disulfides should provide a view of the transient structural modifications that the enzyme experiences during the activation process. Finally, interaction with thioredoxin and with the oxidized form of the cofactor which inhibits activation should provide a complete picture of all the structural rearrangements of this very complex activation process.

ACKNOWLEDGMENT

We thank Irmgard Kurland for linguistic corrections.

REFERENCES

1. Abate, C., Patel, L., Raucher, F. J., and Currran, T. (1990) *Science 249*, 1157−1161.
2. Xanthoudakis, S., Miao, G. G., and Curran, T. (1994) *Proc. Natl. Acad. Sci. U.S.A. 91*, 23−27.
3. Qin, J., Clore, G. M., Kennedy, W. M., Huth, J. R., and Gronenborn, A. M. (1995) *Structure 3*, 289−297.
4. Qin, J., Clore, G. M., Kennedy, W. P., Kuszewski, J., and Gronenborn, A. M. (1996) *Structure 4*, 613−620.
5. Hampton, M. B., and Orrenius, S. (1998) *Biofactors 8*, 1−5.
6. Sen, C. K. (1998) *Biochem. Pharmacol. 55*, 1747−1758.
7. Danon, A., and Mayfield, S. P. (1994) *Science 266*, 1717−1719.
8. Levings, C. S., and Siedow, J. N. (1995) *Science 268*, 695−696.
9. Buchanan, B. B. (1991) *Arch. Biochem. Biophys. 288*, 1−9.
10. Jacquot, J.-P., Lancelin, J.-M., and Meyer, Y. (1997) *New Phytol. 136*, 543−570.
11. Villeret, V., Huang, S., Zhang, Y., Xue, Y., and Lipscomb, W. N. (1995) *Biochemistry 34*, 4299−4306.
12. Hatch, M. D. (1987) *Biochim. Biophys. Acta 895*, 81−106.
13. Miginiac-Maslow, M., Issakidis, E., Lemaire, M., Ruelland, E., Jacquot, J.-P., and Decottignies, P. (1997) *Aust. J. Plant Physiol. 24*, 529−542.
14. Crétin, C., Luchetta, P., Joly, C., Decottignies, P., Lepiniec, L., Gadal, P., Sallantin, M., Huet, J.-C., and Pernollet, J.-C. (1990) *Eur. J. Biochem. 192*, 299−303.
15. Decottignies, P., Schmitter, J.-M., Miginiac-Maslow, M., Le Maréchal, P., Jacquot, J.-P., and Gadal, P. (1988) *J. Biol. Chem. 263*, 11780−11785.
16. Issakidis, E., Miginiac-Maslow, M., Decottignies, P., Jacquot, J.-P., Crétin, C., and Gadal, P. (1992) *J. Biol. Chem. 267*, 21577−21583.
17. Issakidis, E., Saarinen, M., Decottignies, P., Jacquot, J. P., Cretin, C., Gadal, P., and Miginiac-Maslow, M. (1994) *J. Biol. Chem. 269*, 3511−3517.
18. Riessland, R., and Jaehnicke, R. (1997) *Biol. Chem. 378*, 983−988.
19. Ruelland, E., Lemaire-Chamley, M., Le Marechal, P., Issakidis-Bourguet, E., Djukic, N., and Miginiac-Maslow, M. (1997) *J. Biol. Chem. 272*, 19851−19857.
20. Studier, F. W., and Moffat, B. A. (1986) *J. Mol. Biol. 189*, 113−130.
21. Sanger, F., Nicklen, S., and Coulson, A. R. (1977) *Proc. Natl. Acad. Sci. U.S.A. 74*, 5463−5467.
22. Schägger, H., and von Jagow, G. (1987) *Anal. Biochem. 166*, 368−379.
23. de Lamotte-Guéry, F., Miginiac-Maslow, M., Decottignies, P., Stein, M., Minard, P., and Jacquot, J.-P. (1991) *Eur. J. Biochem. 196*, 287−294.
24. Otwinowski, Z. (1993) *Proceedings of the CCP4 Study Weekend*, pp 56−62, Daresbury Laboratories, Warrington, U.K.
25. Ruelland, E., Johansson, K., Decottignies, P., Djukic, N., and Miginiac-Maslow, M. (1998) *J. Biol. Chem. 273*, 33482−33488.
26. Sali, A. (1995) *Mol. Med. Today 1*, 270−277.
27. Navaza, J. (1994) *Acta Crystallogr. 50*, 157−163.
28. Brünger, A. T., Adams, P. D., Clore, G. M., DeLano, W. L., Gros, P., Grosse-Kunstleve, R. W., Jiang, J. S., Kuszewski,

J., Nilges, M., Pannu, N. S., Read, R. J., Rice, L. M., Simonson, T., and Warren, G. L. (1998) *Acta Crystallogr. D54*, 905−921.
29. Cowtan, K. (1994) *Joint CCP4 and ESF-EACBM Newsletter on Protein Crystallography*, Vol. 31, pp 34−38, Daresbury Laboratory, Warrington, U.K..
30. Jones, T. A., Zou, J. Y., Cowan, S. W., and Kjeldgaard, M. (1991) *Acta Crystallogr. 47*, 110−119.
31. Murshudov, G. N., Vagin, A. A., and Dodson, E. J. (1997) *Acta Crystallogr. D53*, 240−255.
32. Lamzin, V. S., and Wilson, K. S. (1993) *Acta Crystallogr. D49*, 129−147.
33. Collaborative Computational Project Number 4 (1994) *Acta Crystallogr. D50*, 760−763.
34. Hall, M. D., Levitt, D. G., and Banaszak, L. J. (1992) *J. Mol. Biol. 226*, 867−882.
35. Pai, E. F. (1991) *Curr. Opin. Struct. Biol. 1*, 796−803.
36. Kelly, C. A., Nishiyama, M., Ohnishi, Y., Beppu, T., and Birktoft, J. J. (1993) *Biochemistry 32*, 3913−3922.

BI982876C